
Interpreting a Machine Learning Model for Detecting Gravitational Waves

Mohammadtaher Safarzadeh

Gravitational Astrophysics Laboratory, NASA Goddard Space Flight Center
mtsafarzadeh@gmail.com

Asad Khan

Department of Physics, University of Illinois at Urbana-Champaign
Data Science and Learning Division, Argonne National Laboratory
National Center for Supercomputing Applications, University of Illinois at Urbana-Champaign

E. A. Huerta

Data Science and Learning Division, Argonne National Laboratory
Department of Computer Science, The University of Chicago

Martin Wattenberg

School of Engineering and Applied Sciences, Harvard University

Abstract

We describe a case study of translational research, applying interpretability techniques developed for computer vision to machine learning models used to search for and find gravitational waves. The models we study are trained to detect black hole merger events in non-Gaussian and non-stationary advanced Laser Interferometer Gravitational-wave Observatory (LIGO) data. We produced visualizations of the response of machine learning models when they process advanced LIGO data that contains real gravitational wave signals, noise anomalies, and pure advanced LIGO noise. Our findings shed light on the responses of individual neurons in these machine learning models. Further analysis suggests that different parts of the network appear to specialize in local versus global features, and that this difference appears to be rooted in the branched architecture of the network as well as noise characteristics of the LIGO detectors. We believe efforts to whiten these “black box” models can suggest future avenues for research and help inform the design of interpretable machine learning models for gravitational wave astrophysics.

Keywords: Interpretable AI, Reproducible AI, Black Hole Mergers, Gravitational Waves

1 Introduction

The advent of large scale scientific facilities [Tingay, 2015, Apollinari et al., 2017, LSST Science Collaboration et al., 2009, Albrecht et al., 2019], next generation imaging technology, and supercomputing have enabled remarkable advances in contemporary science and engineering [Gropp et al., 2020, Huerta et al., 2020, Conte et al., 2021]. As these facilities continue to produce scientific datasets with ever increasing precision, volume and velocity, researchers have been empowered to make precision-scale measurements and predictions that are revolutionizing multiple fields: cosmology, agriculture, personalized nutrition, genomics and particle physics [Guest et al., 2018, Huerta et al., 2019, Narita et al., 2020, Guo et al., 2021, Uddin et al., 2019, Chen et al., 2021].

Machine learning (ML) has begun to play an important role in this data-rich environment. Recent successes have ranged from processing gravitational wave data and identify true gravitational wave signals in advanced LIGO data [George and Huerta, 2018a, George and Huerta, 2017, George and Huerta, 2018b,c] to automating the classification of galaxies observed by the Dark Energy Survey and the Sloan Digital Sky Survey [Khan et al., 2018, Khan and Huerta, 2018, Khan et al., 2019], and star cluster images by Hubble [Wei et al., 2020, Whitmore et al., 2021], to mention a few. Neural networks have been a key ML technique used in these projects.

Although neural networks have had many successes, they also have a key drawback when seen as scientific instruments: they often appear as black boxes, since how they make their decisions is unclear. Understanding how these neural networks work would have many general benefits [Doshi-Velez and Kim, 2017]. Information on how neural networks function can help find bugs, inspire potential improvements [Alsallakh et al., 2021], and help calibrate trust in their decisions [Carvalho et al., 2019]. In the context of astrophysics, there is also the potential that examining the features that a network thinks is important can give clues to new science [Ntampaka and Vikhlinin, 2021].

These questions have been investigated in many other contexts, ranging from image classification [Simonyan et al., 2013] to natural language processing [Tenney et al., 2019]. Our goal here is to describe a case study in interpretability, showing how scientists can apply techniques from this literature to a real-world scientific ML system, aimed at a very different domain. Our hope is to demonstrate the value of these techniques generally in the context of applications that involve complex, noisy, heterogeneous and incomplete scientific datasets.

In this article, we use gravitational wave astrophysics as a science driver to explore the inner workings of four different neural network models that have been used for production scale, data-driven gravitational wave detection in advanced LIGO data [George and Huerta, 2018a, George and Huerta, 2017, George and Huerta, 2018b,c, Huerta et al., 2021]. We will refer to these models as the **GW ensemble**.

Our findings on the GW ensemble fall into two main categories. First, we find reassuring evidence that the ML model is based on physically meaningful features. A potential failure mode for an ML model is to pick up on confounding variables—for example, some medical image analysis systems have learned to identify the hospital and department where an image was taken [Zech et al., 2018]. The fact that the GW model appears to focus on features that are intuitive to astrophysicists may increase trust in the system. Second, our explorations shed light on how the architecture of the GW model network may be influencing its computation. For example, the network is divided into two main branches, reflecting the physical architecture of the LIGO detectors. Our investigation suggests these branches have specialized in different ways.

While these results do not come close to a full explanation of the GW ensemble’s decisions, they do provide a framework for understanding how those decisions are made, and can serve as a basis for future investigations of these models. More generally, our findings suggest that existing interpretability methods have reached the point where they may be broadly useful across domains.

2 Detecting gravitational waves: model and data

We describe the ML models and data used in the GW ensemble, and the methods used to understand how these models distinguish between gravitational waves and noise anomalies. Because the domain is deeply technical, we begin with a basic description of the problem at hand, suitable for ML practitioners.

2.1 Machine learning to detect black hole mergers

Physicists have long been interested in “gravitational waves,” ripples in the geometry of the universe caused by very compact objects, e.g., black holes or neutron stars, moving at a fraction of the speed of light. General relativity predicts the existence of these waves—and that they are extremely hard to detect. Confirming their existence was, for decades, a major unsolved problem in experimental physics. One particularly dramatic type of astronomical event is the merger of two black holes that will create ripples in space-time with large enough amplitude to be detected by detectors such as advanced LIGO. When two black holes merge, they orbit at decreasing distance and increasing speed,

until they collide. The resulting gravitational waves should, theoretically, increase in magnitude and frequency until the point of collision—then cease.

Dramatic as these astronomical events are, they occur so far from the earth that the resulting waves are still weak compared to ambient noise. The LIGO detectors were designed to detect the presence of gravitational waves, and consist of two geographically separated sites, Hanford (Washington State) and Livingston (Louisiana). To confirm an observation of a binary black hole merger, physicists need to solve a basic classification problem: analyze time series from the Hanford and Livingston detectors, and classify whether the data includes a gravitational wave signal.

As a ML task, the problem can be abstracted as follows. The input consists of two vectors of real numbers, which correspond to time series from the two detectors for a small period of time. The output will be a vector of the same length, but consisting of numbers between 0 and 1, corresponding to a measurement of how likely it is that a black hole merger is happening at that instant. ML models for this task are typically trained on simulated waveforms (verified binary merger events are scarce) combined with real background noise (which is all too plentiful).

2.2 Model and data

The ML ensemble we use in this study was introduced in Huerta et al. [2021]. As described below, these models share the same architecture and only differ in their weight initialization. The modeled waveforms we used to train them describe a 4-D signal manifold that encompasses the masses and individual spins of the binary components of quasi-circular, spinning, non-precessing binary black hole mergers, namely, (m_1, m_2, s_1^z, s_2^z) . This is the same parameter space employed by those trained with modeled waveforms that describe the physics of quasi-circular, spinning, non-precessing binary black hole mergers, i.e., the same 4-D signal manifold of traditional, template-matching pipelines used for gravitational wave searches [Usman et al., 2016, Nitz et al., 2018, Cannon et al., 2021].

These modeled waveforms were combined with advanced LIGO noise to expose these models to a diverse set of astrophysical scenarios encoding time and scale invariance, i.e., these ML models may identify gravitational waves irrespective of their signal to noise ratio or location in the input time-series advanced LIGO strain. Furthermore, these models were tested using hours-, weeks- and a month-long advanced LIGO dataset to quantify their ability to identify real events and discard noise anomalies. The studies presented in Huerta et al. [2021] showed that this ensemble of 4 ML models can concurrently process data from Hanford and Livingston, correctly identifying all binary black hole mergers reported throughout August 2017 with no misclassifications.

To enable other researchers to reproduce these studies, these AI models were released through the Data and Learning Hub for Science. To facilitate the use of these models we have demonstrated how to connect DLHub with the HAL GPU-cluster at the National Center for Supercomputing Applications, and do inference by using funcX as a universal computing service. Using the framework DLHub-funcX-HAL, we showed that it is possible to process a month’s worth of advanced LIGO noise within 7 minutes using 64 NVIDIA V100 GPUs. It is worth contextualizing these results with other studies in the literature. For instance, the first class of neural networks for gravitational wave detection [George and Huerta, 2018a, George and Huerta, 2017, George and Huerta, 2018b] were tested using 4096 second long advanced LIGO data segments, reporting one misclassification for every 200 seconds of searched data. More sophisticated neural networks have been developed to test days- and weeks-long advanced LIGO data, reporting one misclassification for every 2.7 days of searched data [Wei et al., 2021], and one misclassification for every month of searched data [Chaturvedi et al., 2022]. In brief, the ML ensemble we used in this study represents a class of neural networks that are adequate for accelerated, data-driven gravitational wave detection at scale. The key components of our ML models and data encompass:

Modeled waveforms Our ensemble of four ML models was trained with 1.1 million waveforms produced with the SEOBNRv3 approximant [Pan et al., 2014]. These waveforms, sampled at 4096 Hz, describe quasi-circular, spinning, non-precessing, binary black hole mergers with total mass $M \in [5M_\odot, 100M_\odot]$, mass-ratios $q \leq 5$, and individual spins $s_{\{1,2\}}^z \in [-0.8, 0.8]$. These 1-second long waveforms describe the late-inspiral, merger and ringdown phases.

Advanced LIGO noise The modeled waveforms described above are whitened and linearly mixed with 4096-second long advanced LIGO Hanford and Livingston noise data segments obtained from the Gravitational Wave Open Science Center [Vallisneri et al., 2015]. The start GPS time of each

of these segments is: 1186725888, 1187151872, and 1187569664. None of these data segments contained gravitational wave signals. The ground truth labels were encoded in a binary fashion such that time-steps after the merger are classified as noise [labelled 0], and all preceding time-steps in the 1 second long window are classified as waveform strain [labelled 1]. Hence the transition from 1s to 0s indicates the location of the merger.

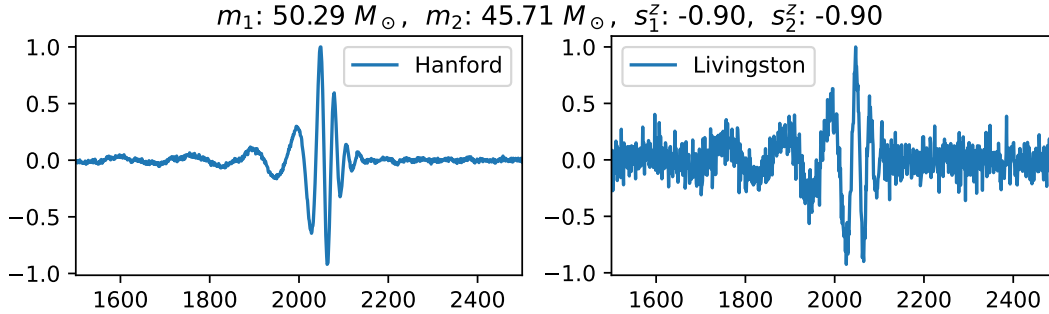


Figure 1: **Input data for training:** The panels show whitened waveforms with advanced LIGO noise using Hanford (left panel) and Livingston (right panel) strain data. The waveforms represent different configurations our neural networks are exposed to during the training stage. The example shown here is the GW of a binary black hole with component masses $m_1 = 50.29M_\odot$, $m_2 = 45.71M_\odot$ and individual spins $s_1^z = s_2^z = -0.9$ that has been whitened with a PSD representative of O2 advanced LIGO noise and then linearly combined with whitened O2 noise.

To train the models, as described in Huerta et al. [2021], co-authors of this article created a set of modeled waveforms, selected a batch of advanced LIGO noise to estimate a power spectral density (PSD), and then use this PSD to whiten both modeled waveforms and noise so that these may be linearly added at will to expose our AI models to modeled signals that are contaminated with multiple noise realizations and signal-to-noise ratios during training. Figure 1 presents a sample case in which a modeled waveform that describes a black hole binary with component masses $m_1 = 50.29M_\odot$, $m_2 = 45.71M_\odot$ and individual spins $s_1^z = s_2^z = -0.9$ has been whitened with a PSD representative of O2 advanced LIGO noise and then linearly combined with whitened O2 noise. At inference, our AI models process whitened advanced LIGO data at scale and produce a typical response function that differentiates real events from noise anomalies.

2.3 Neural network architecture

The architecture of each model in the GW ensemble consists of two branches and a shared tail, as shown in Figure 2. The two branches are modified WaveNets [van den Oord et al., 2016] processing Livingston and Hanford strain data separately. The key components of a WaveNet architecture are dilated causal convolutions, gated activation units, and the usage of residual and skip connections. Since ours is a classification task instead of an autoregressive one, e.g., waveform generation, we turn off the causal padding in the convolutional layers. We use filter size of 2 in all convolutional layers and stack 3 residual blocks each consisting of 11 dilated convolutions so that the receptive field of each branch > 4096 . The outputs from the two branches are then concatenated together and passed through two more convolutional layers of filter-size 1. Finally a sigmoid activation function is applied to ensure that the output values are in the range $[0, 1]$. The complete network structure was introduced in [Huerta et al., 2021].

We trained multiple ML models with this architecture using the same training datasets (modeled waveforms & advanced LIGO noise) but different weight initialization. We then selected 4 models out of our training suite (via a process to optimize ensemble accuracy) and wrote post-processing software that looks at the combined output of this ensemble. We only label noise triggers as candidate events when the response of all four models is consistent with an event whose threshold for detectability is above a given threshold, as described in detail in Huerta et al. [2021].

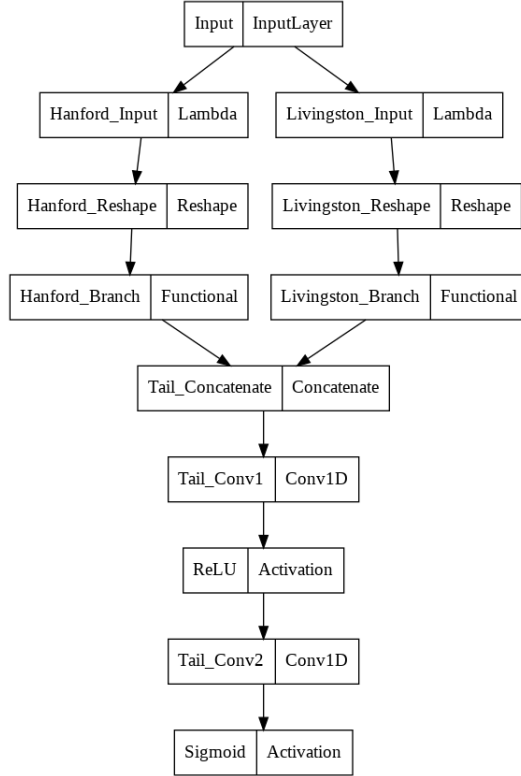


Figure 2: **Branched architecture:** This two branch neural network structure is used to concurrently process Hanford and Livingston advanced LIGO data. The architecture of each branch closely follows that of WaveNet model [van den Oord et al., 2016].

3 Visualization and interpretation of the GW ensemble

The GW ensemble is a successful production system that has proven useful to scientists. As described above, it is accurate and efficient. Yet it is unclear how it achieves this success. The goal of our investigation is to show how techniques that have been developed for neural nets in other fields (primarily machine vision) can be used to shed light on different aspects of the ensemble.

We present three types of results, namely, sensitivity maps to peer into the response of our ML models to a variety of input data; scientific visualizations that showcase the response of our models to second-long input datasets; and activation maximization studies which suggest that individual neurons within the GW ensemble respond especially strongly to signals that resemble part or all of modeled merger events.

3.1 Activation maximization

Background:

A natural question is whether individual neurons respond to characteristic types of signals. One way to investigate this question is to look for signals that maximally activate a particular neuron [Erhan et al., 2009]. In the special case of a neuron that is computing a class score, this is roughly equivalent to finding an input signal that the network thinks is “most likely” to be of a certain class.

Conceptually, one may think of these maximally-activating signals as templates that the network is looking for. In the case of convolutional neural networks used in computer vision, one often sees a hierarchy of such templates. Lower-level neurons pick out simple signals, such as edges, and higher-level neurons seem to respond best to concepts such as an eye, or an entire dog [Cammara et al., 2020]. While this technique has largely been applied to 2D convolutional networks, although it has been applied to EEG data (via the frequency domain) in the case of Ellis et al. [2021].

Application to time-series gravitational wave data:

To investigate the GW ensemble, we chose a middle position (element 2000) in the data window, and synthesized signals that maximize the neuron activations at this specific timestamp position for different layers. To understand aggregate activity, we maximized total activation in a given layer. We computed maximizing signals for individual neurons as well, which gave similar results.

We perform the maximization procedure 10 times for each layer. In all cases we have started with pure Gaussian noise with mean zero and standard deviation of 0.02. For all activation maximization studies in all of the layers we have adopted a learning rate of 0.5 with momentum 0.9 using Adam optimizer for performing the calculations necessary to seek a maximizing signal. We use $L = |1 - x_n|^2$ as a loss, where x_n is the value of the activation of neuron n , and stop when $L < 0.01$.

Results:

Results from the first 10 layers for Hanford branch are shown in Figure 3. We see that the maximally activating patterns are far from random noise, instead resembling different gravitational waveform-like signals. (Recall the training examples in Figure 1.) Neurons in the first layer seem maximally activated by spikes, and as we move through deeper layers the signals become longer and more complex. The results are similar for the Livingston branch in these early layers. This pattern seems like a one-dimensional analogue of the pattern seen in networks aimed at computer vision [Erhan et al., 2009].

Figure 4 shows the activation maximizing signal for the last layer of the network. We notice that the result for the Hanford branch resembles a denoised, whitened waveform with the merger event very well defined. One possible interpretation of this analysis is that the the Hanford branch specializes in searching for and identifying local features that describe the merger event. On the other hand, the Livingston branch seems to react more sharply to noise contaminated waveform-like signals over extended periods of time, not just around the merger event. Potentially related aspects of the Hanford and Livingston branches manifest themselves in similar fashion in the studies we present below.

3.2 Visualizing activations

Method:

A direct method of visualizing the response of a neural network is to show the activations of all neurons in a single image. In the case of the GW ensemble, this means displaying 12,914,688 activations in a single diagram.

While this may seem like an overwhelming number, if we allocate one pixel per neural unit, and use color to encode activation level, it becomes feasible to create a holistic view of the the response in every layer at once. There are two main questions that such a visualization can answer. One is, can we see any differences between how the network processes signals that contain a gravitational wave, versus one that is pure noise? The second is, are there systematic differences between the two branches of the network?

Results:

As a baseline, we begin by visualizing the response of the network to a non-merger event. The left panel in Figure 5 shows the response of all the activation layers of one of the WaveNet models in the ensemble to advanced LIGO noise in the absence of signals.

Next, we conducted a similar analysis for the binary black hole merger GW170814, and present corresponding results in Figure 6. Pair-wise comparisons between Figures 5 and 6 show that our neural networks respond very differently, across all layers, when there is a signal in the data. The top layers show activations at the location of the merger event, gradually spreading out and branching as we move towards deeper layers. Although this result is not surprising, it provides some validation for the model and the visualization technique.

As a final exploration, Figure 7 visualizes the response of the network to a “glitch,” i.e., a noise anomaly resembling a gravitational wave. The layers involved in the detection behave differently from when a real signal is present as shown in Figure 6. One obvious difference is the fuzziness of the activations in the early layers in detecting the merger event. One interpretation of this behavior is that it relates to the uncertainty of network as to where exactly the merger event is taking place.

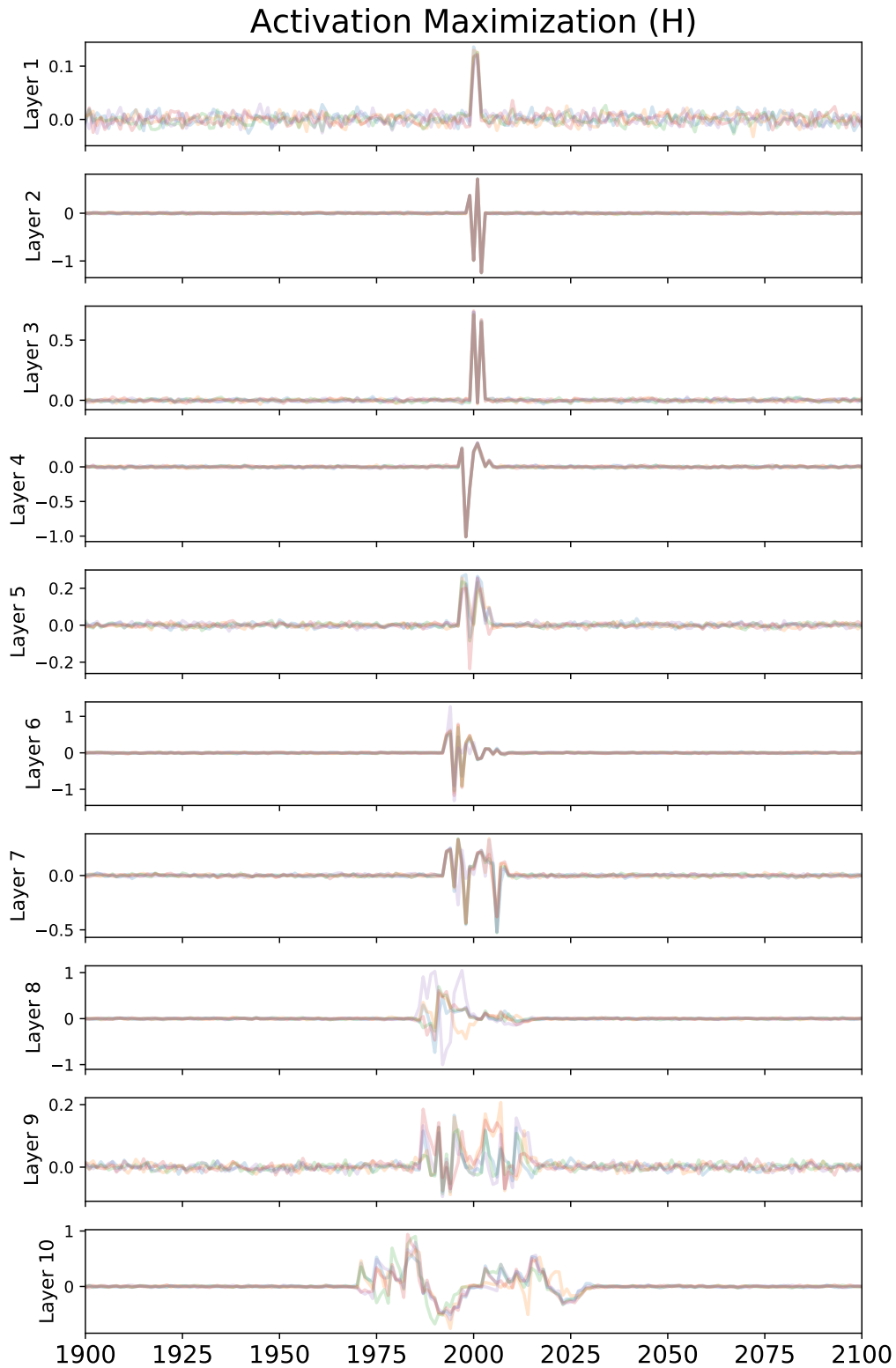


Figure 3: **Activation maximization in shallow layers:** Each panel presents how a single neuron's activation is maximized when we input random Gaussian noise with mean zero and standard deviation of 0.02. We repeat this procedure 5 times, using learning rate of 0.1 and stochastic gradient descent optimizer with momentum 0.9.

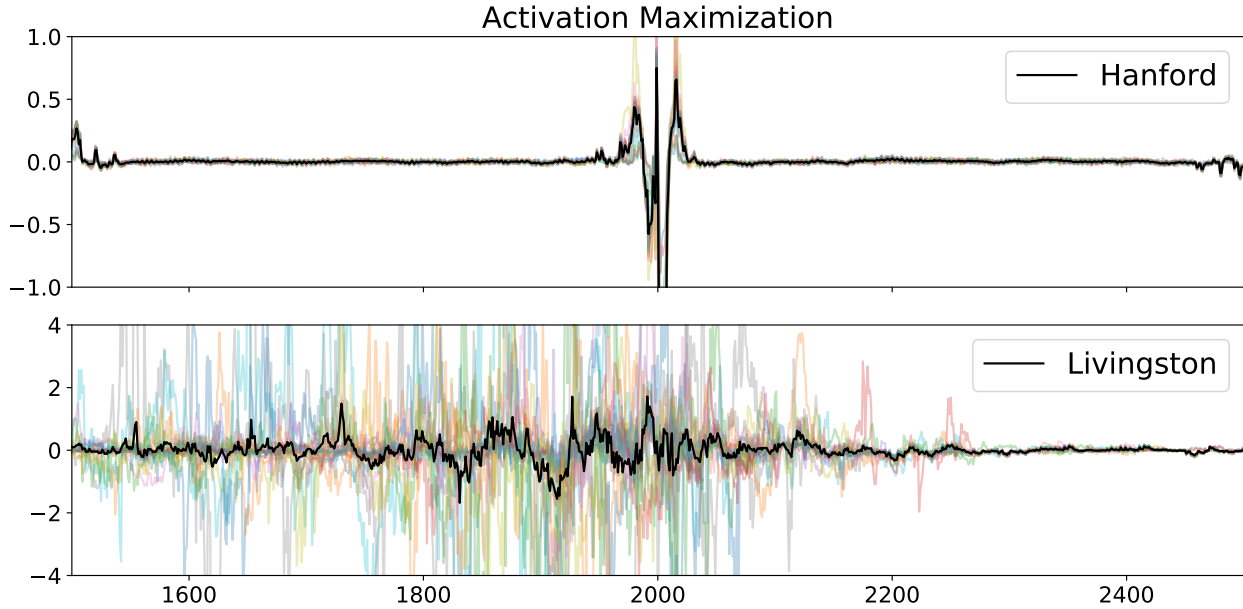


Figure 4: **Activation maximization in last layer:** Same as Figure 3, but now for the last activation layer of the network. The activation maximization is performed 20 times, the result of each is shown with a colored line. All the 20 tries have the initial condition of random Gaussian with mean zero and standard deviation of 0.02. The black line shows the average of the 20 tries. Top (bottom) panel shows the result for the Hanford (Livingston) branch of the network. (The difference between branches is a consistent theme in our analysis.) We have adopted a learning rate of 0.5 with momentum 0.9 using Adam optimizer for performing the gradient descent calculations. We refer the readers to the movie in this [YouTube link](#) showing the process of finding the activation maximizing signal from pure noise.

We can make additional observations based on these visualizations: (i) a set of layers (from 20 through 45) in the Livingston branch remain very active, though with rather different behaviour, to all inputs we consider, i.e., pure noise, real signal and glitch, as shown in Figures 5- 7, respectively. What we learn from these results is that the Livingston branch seems to look for global features in the input, in similarity to the findings we reported above on activation maximization; (ii) the response of the Hanford branch to noise anomalies or gravitational wave signals is sharper and more concentrated than that of the Livingston branch, as shown by layers 5 through to 35 in Figures 6 and 7. Again, this is consistent with our findings above in which the Hanford branch seems to be maximally activated by more localized features.

3.3 Sensitivity Maps

Background:

A basic technique for understanding the features relevant to a classification decision is to examine the gradient of the class scores, or equivalently the Jacobian of the final layer. Conceptually, the gradient tells us, for each feature, how much an infinitesimal change in that feature will affect the class score. A common hypothesis is that if the network is particularly sensitive to a given attribute, then that attribute is playing an important role in the classification. This technique, along with close variants, has been widely used in the machine vision community [Simonyan et al., 2013, Smilkov et al., 2017, Sundararajan et al., 2017, Selvaraju et al., 2017, Montavon et al., 2019]. It has also been applied in the context of time series [Ismail et al., 2020, Fawaz et al., 2019]

Application to time-series gravitational wave data:

Recall the architecture of the ML model: In the case of the WaveNet models we use for this study [Huerta et al., 2021], both the input and output layers are vectors in 4096 dimensions. The

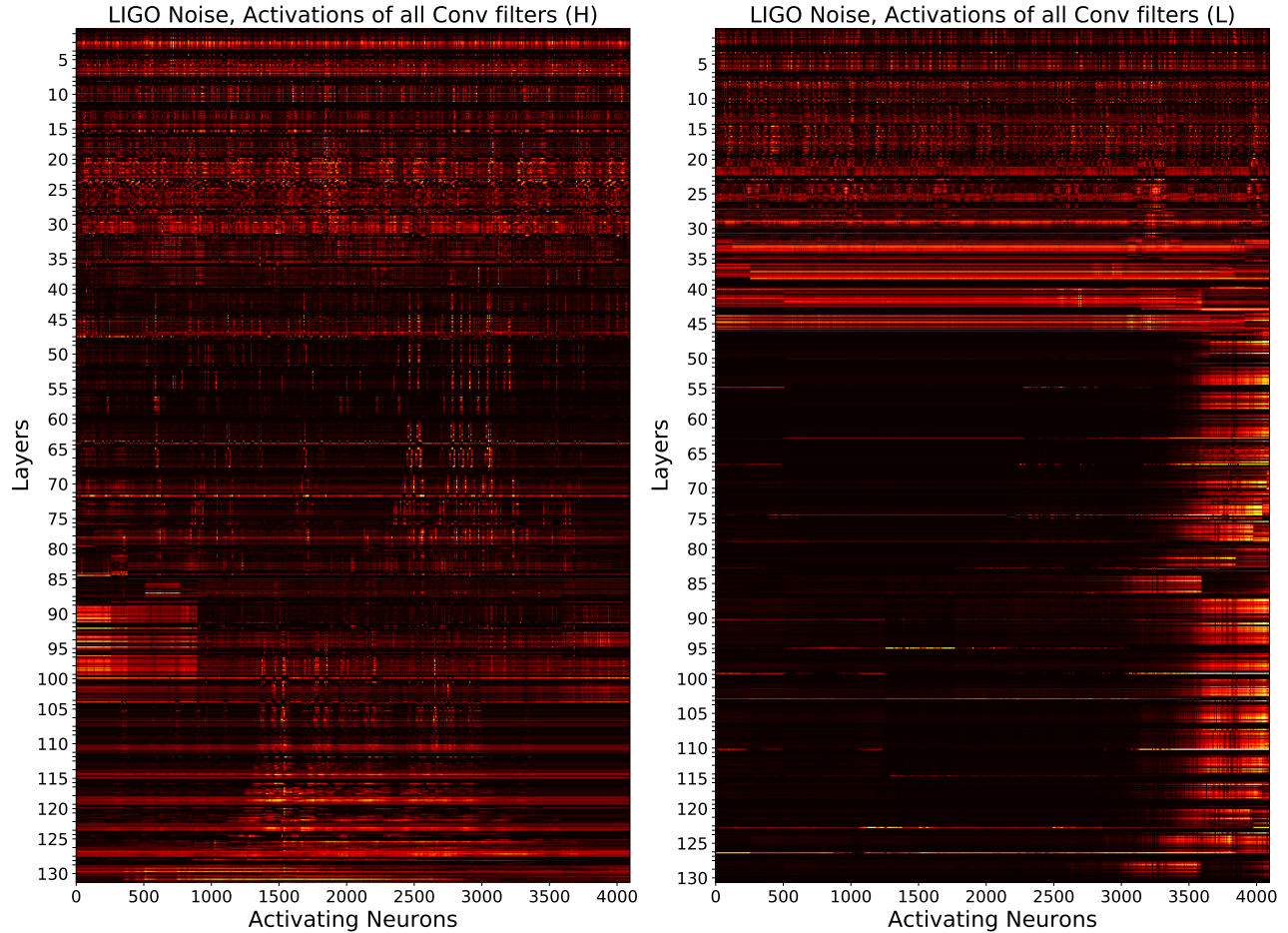


Figure 5: **Visualization of activations for pure noise:** Each of our ML models has two branches that concurrently process Hanford and Livingston strain data. These panels show the response of the convolutional layers in each of these networks from the shallow layers (top part) to the very last layers (deepest layers) for the Hanford and Livingston branches. We used advanced LIGO data from the second observing run to produce this visualization.

neurons in the output layer report the probability of the presence of a gravitational wave prior to that neuron, and zero otherwise. For example, if the input data contains a gravitational wave signal that describes a binary black hole whose merger occurs at timestep 3000 (in the 4096-D input), then the output neurons will report values close to 1 for all the neurons prior to timestep 3000 and zero otherwise. By computing the Jacobian between all the neurons in the output and input layer, we arrive at a 4096×4096 matrix. Following the work cited above, we interpret this matrix as a “map” of the sensitivity of each of the 4,096 separate classifications to each of the 4096 coordinates of the input vector.

Results for a signal of advanced LIGO noise:

As a baseline, we first created a sensitivity for a signal containing no merger event, whitened advanced LIGO noise inputs. Figures 8 and 9 shows four panels that correspond to the Jacobian of each of our four ML models for the Hanford and Livingston branches, respectively. The x -axis in each panel shows the input waveform (in this case input noise), while the y -axis shows the output neuron.

We notice a clear cut difference between the H and L branches, namely, there are large swaths of dormant neurons in the H branch for several ML models, while the L branch in our models has solid activity throughout. This, again, is consistent with previous findings in that the L branch is searching for features in a global manner, while the H branch has a more narrow scope of feature identification.

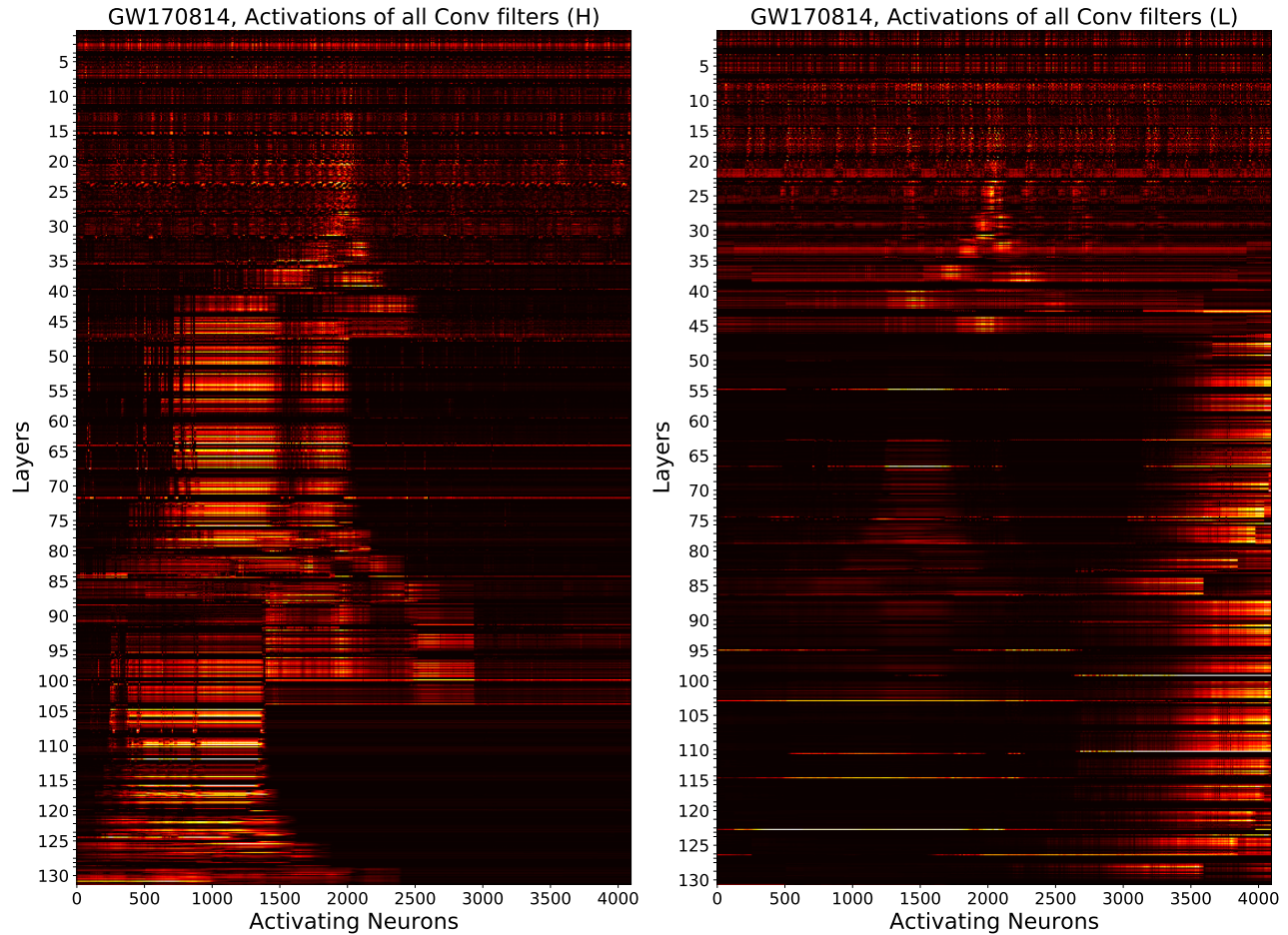


Figure 6: **Visualization of activations for GW170814:** Same as Figure 5, but now for a real gravitational wave source, GW170814. We notice a sharp, distinct response of this network for a signal whose merger is located around timestep 2000. We refer the readers to the movie in this [YouTube link](#) showing how neurons in different layers are activated by the passage of a GW in the time series signal.

This sensitivity map offers one more useful observation. Note the prominent dark corners at lower left and upper of the images. These correspond to zero sensitivity. Indeed, a simple calculation from the architecture of the network shows that it is impossible for a final-layer neuron at one end of the signal to be affected by input data at the other end. In other words, the field of view of neurons does not always cover the entire signal.

Results for GW170818:

Having analyzed sensitivity for a signal without a merger, we turn to the case of a signal with a verified event: a binary black hole merger known as GW170818. This event was chosen since it was particularly strong, and thus we may observe a sharp response in our ML models.

Comparisons between Figures 8 and 10 show that our ML models indeed have a visibly different response when the input data contains a real signal. First, the diagonal line we observe in all panels in Figure 8 is not as prominent when the input data contains real signals.

Second, we observe two new lines or bands, one vertical at timestep 3,000, and one horizontal at location 3,000. The horizontal line indicates that output at the location of the merger is sensitive to the entire input signal. The vertical line about the location 3,000 suggests that all the neurons in the last layer are sensitive to information residing at timestep 3,000 in the input signal, meaning all the neurons in the last layer are sensitive to the merger event. We observe similar patterns when

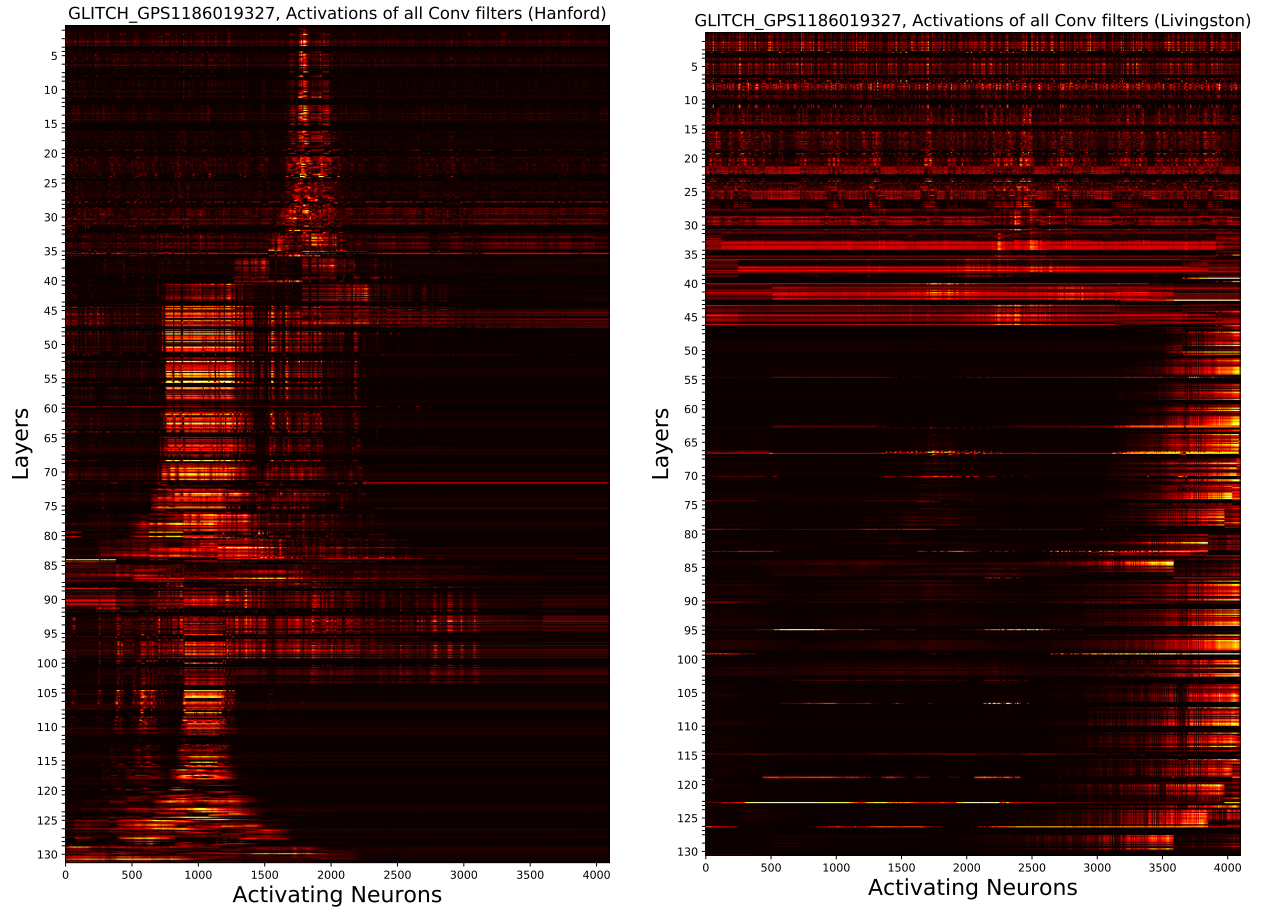


Figure 7: **Visualization of activations for a glitch** Unlike for the case of a real signal, the reaction of the network to a glitch is different in its top (early) layers: we observe a sense of fuzziness indicative of the uncertainty in the network as to where the merger event is taking place.

we make pair-wise comparisons of Figures 9 and 11, except we do not see a clear vertical line in Figure 11. On the other hand, what remains the same is that the Hanford and Livingston branches respond differently to real gravitational wave signals. The Livingston branch seems to search for global features in the input data, while the Hanford branch appears to focus on localized features of the merger event.

To rule out the possibility that the particular timestep we chose was somehow special, we conducted additional experiments in which we manually shifted the location of the merger event, using a different start time to clip the advanced LIGO segment containing this signal and then feeding it into our models. We observed that the time shift we used to clip this input data segment coincided with the actual location of these horizontal and vertical lines. We also used several synthetic signals that we injected in advanced LIGO noise and repeated these experiments several times. In all these experiments we observed a strikingly similar feature response.

4 Discussion

The results of the three experiments suggest several hypotheses about how the GW ensemble functions. We describe how individual units in the network appear to respond in an intuitive way to aspects of the incoming signal. At the architectural level, the two-branched form of the network seems to lead to an unexpected separation of concerns: one branch seems to focus on more local features, another on denoising and global features.

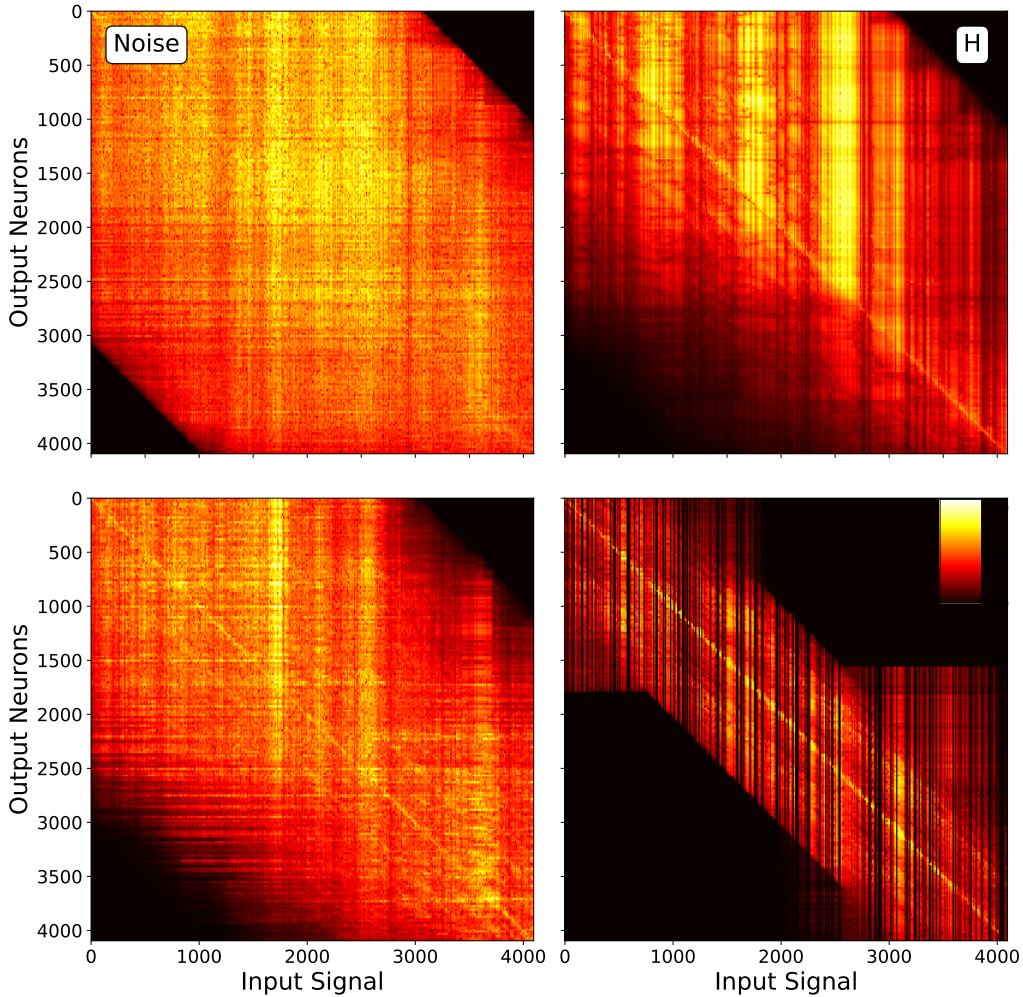


Figure 8: **Jacobian for advanced LIGO noise inputs of Hanford branch:** The four panels present the Jacobian, computed using the last layer of each of the four models in our AI ensemble, when we feed advanced LIGO noise. We identify two recurrent features in these panels: (i) a diagonal line, which indicates that the neurons in the final layer are always sensitive to the corresponding input neuron in the absence of a real signal; (ii) the dark corner regions in the panels are indicative of the restricted field of view of the neurons in the last layer with respect to the input signal. Neurons in the deeper layers have wider field of view.

4.1 Signals and individual neural responses

At a basic level, all three visualization techniques reveal that these neural networks may be less mysterious than they appear. All of the activation layers of the network react differently when a signal is present versus pure noise. When there is no signal in the input data, the neurons in the last layer are mostly sensitive to the corresponding neuron in the input layer. In the presence of a signal in the data, the neuron in the last layer around the merger event becomes sensitive to the entire input time-series data.

Furthermore, the type of signal matters. The network reacts differently to stellar mass vs heavier binary black hole mergers. We consistently noticed that more neurons are actively involved in detection of lighter systems, as opposed to their heavier counterparts. Perhaps if a signal is harder to detect, larger parts of the neural net will be involved in the classification task. Finally, each of the

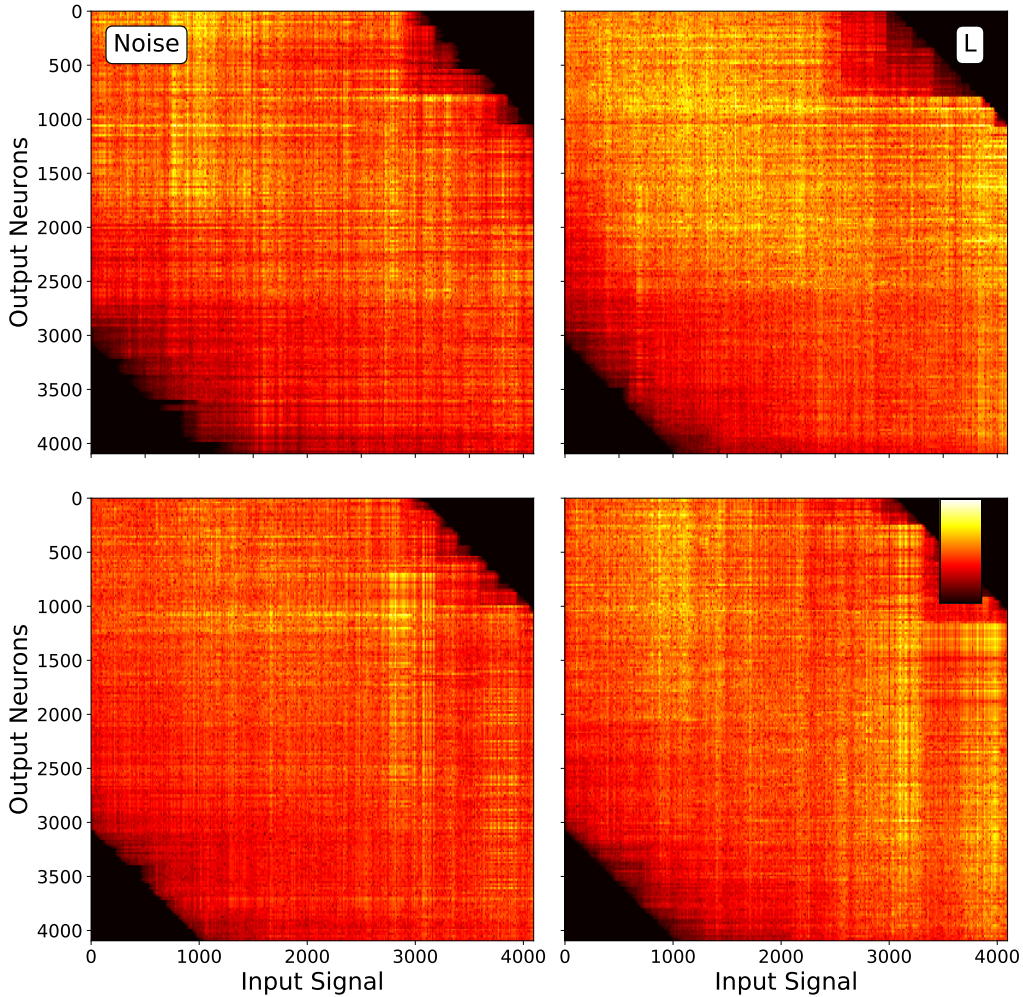


Figure 9: **Jacobian for advanced LIGO noise inputs:** Same as Figure 8, but for the Livingston branch of each of the four models.

four models react differently to the input data, which indicates each iteration of training of the model has led to slight differences in how a net has learned to tell apart signals from noise anomalies.

Activation maximization experiments suggest that channels and individual neurons are sensitive to “template” signals that resemble part or whole waves, with a distinct visual similarity to training data examples. Moreover, early layers are activated by the presence of a simple spike, while deeper layers are activated by more complicated signal. Visualizing activations and sensitivity maps directly shows that the network seems to find the moment of a black hole merger especially salient. All three experiments indicate a progression from very local to more global feature extraction. These results seem intuitive, and match similar results from computer vision networks.

4.2 Branch specialization

Beyond these basic observations, however, our visualizations point to an unexpected finding, painting a scenario in which the two branches of our neural network have specialized for somewhat different tasks. The Livingston branch seems to focus on global features of waveform signals. Synthetic signals designed to optimize the Livingston response generally were much noisier than equivalent signals for the Hanford branch, and seemed to span a wider time scale. We hypothesize the Livingston branch may have a special role in identifying global, longer time-scale features of waveform signals.

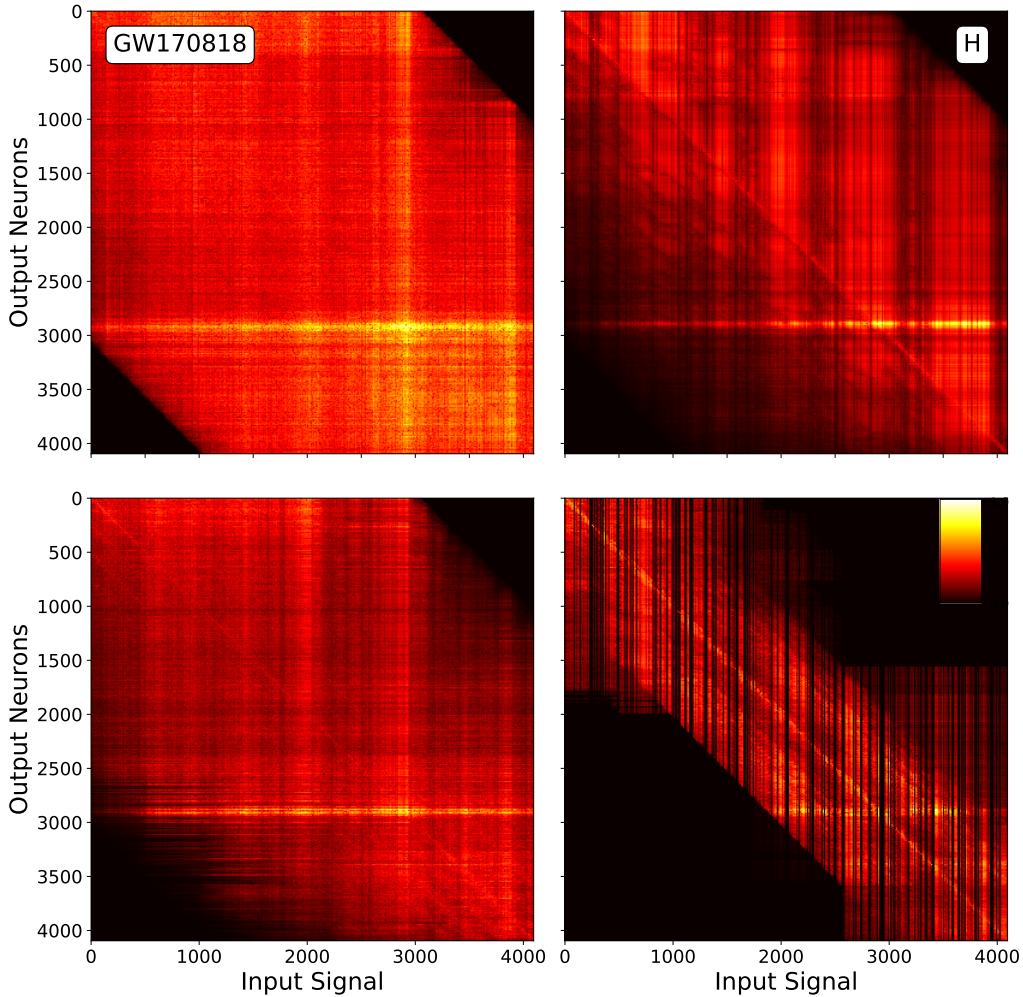


Figure 10: **Jacobian for GW170818:** Same as Figure 8, but now for the merger event GW170818. These results show that when the ML models process advanced LIGO data containing real events, output neurons in the last layer of these models respond in a distinct manner when they identify features that are consistent with the merger of binary black holes. These panels contain that information in the sharp vertical and horizontal lines at output neuron and timestep 3,000, which coincide with the merger of GW170818.

Meanwhile, the Hanford branch appeared to focus on shorter-time events that were smoother. Working in tandem, these branches learn to identify key features that define the physics of binary black hole mergers and which are not present in other types of noise anomalies.

This difference between branches raises a number of questions. Branch specialization has been observed to occur spontaneously[Voss et al., 2021] simply due to architectural separation within a neural network. In the case of the GW ensemble, however, there is the additional factor that the two branches are given signals that, although similar, have slightly different noise characteristics. Understanding the relation between the differences in training data and the resulting specialization seems like an important area for future research. Furthermore, understanding the emergent differences in processing may help in evaluating future versions of the network, or even choosing which trained networks to include in an ensemble.

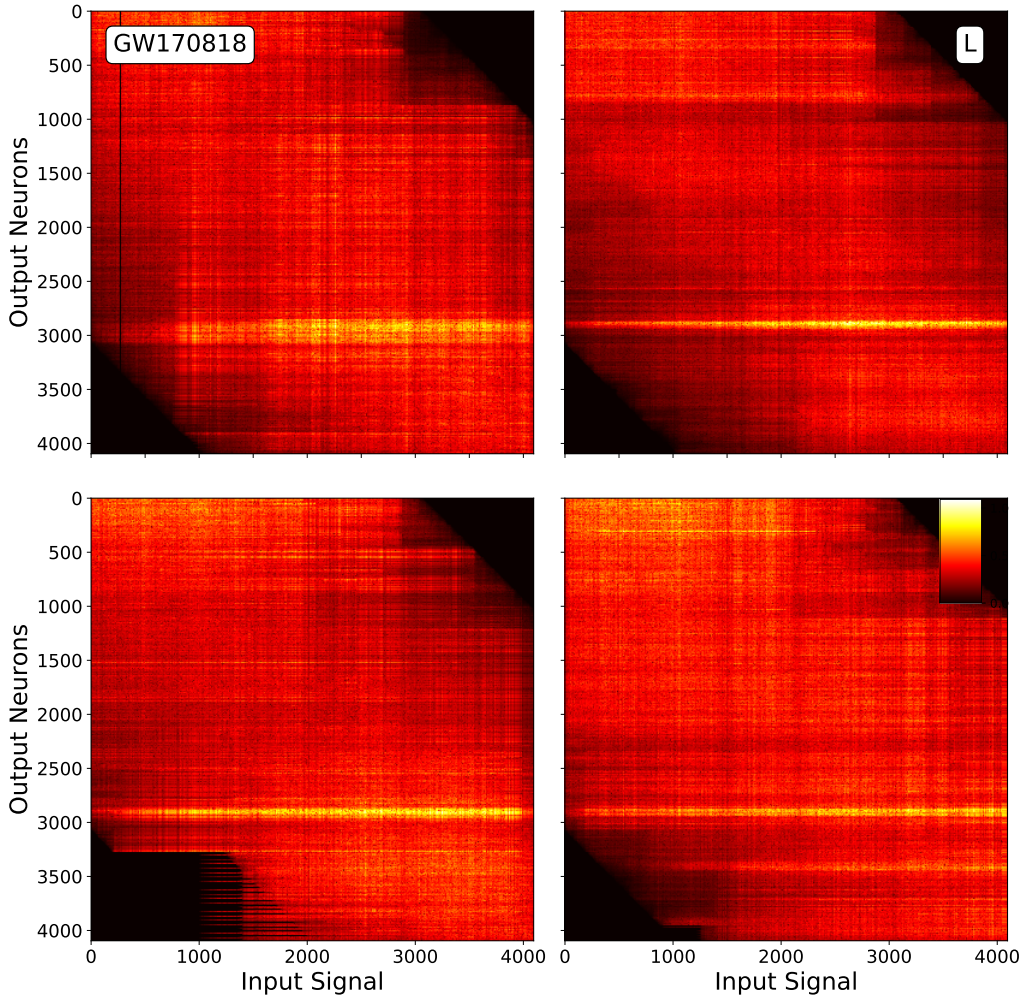


Figure 11: **Jacobian for GW170818**: Same as Figure 10, but for the Livingston branch of each of the four models.

5 Conclusion

We draw three general conclusions from our interpretability experiments. First, there is value to this type of translational research: although many of the techniques we have applied were first developed in other domains, they appear to shed light in our context as well. Moreover, all three techniques paint a consistent picture of a network whose branches are performing different types of computations, and which responds to increasingly global features as layer depth increases.

The second conclusion is that there is significant room for new research based on these initial findings. One natural direction is looking for ways to modify the basic network architecture. For example, in the current models the Jacobian investigation brings up the fact that some units in the final layer are not sensitive to the entire field; however, it would be straightforward to change the architecture to avoid this. At a deeper level, the activation visualizations indicate that in some cases a large portion of the network seems to respond similarly to signals with and without an event; a close examination of this phenomenon might suggest ways to compress or prune the network.

Finally, our visualizations raise additional avenues for interpretation. In particular, we have hypothesized that the specialization of the two branches relates at least partly to the difference in baseline noise levels in the two detectors. Understanding how differences in data distribution might affect spontaneous branch specializing is an appealing question. From a practical standpoint, it would be

useful to understand whether this type of specialization contributes positively to performance or has a neutral or negative effect.

6 Acknowledgements

We are thankful to David Bau for careful reading of our paper before submission. A.K. and E.A.H. gratefully acknowledge National Science Foundation (NSF) awards OAC-1931561 and OAC-1934757. E.A.H. gratefully acknowledges the Innovative and Novel Computational Impact on Theory and Experiment project ‘Multi-Messenger Astrophysics at Extreme Scale in Summit’. This material is based upon work supported by Laboratory Directed Research and Development (LDRD) funding from Argonne National Laboratory, provided by the Director, Office of Science, of the U.S. Department of Energy under Contract No. DE-AC02-06CH11357. This research used resources of the Argonne Leadership Computing Facility, which is a DOE Office of Science User Facility supported under Contract DE-AC02-06CH11357. This research used resources of the Oak Ridge Leadership Computing Facility, which is a DOE Office of Science User Facility supported under contract no. DE-AC05-00OR22725. This work utilized resources supported by the NSF’s Major Research Instrumentation program, the HAL cluster (grant no. OAC-1725729), as well as the University of Illinois at Urbana-Champaign. We thank NVIDIA for their continued support.

References

- Johannes Albrecht et al. A Roadmap for HEP Software and Computing R&D for the 2020s. *Comput. Softw. Big Sci.*, 3(1):7, 2019. doi: 10.1007/s41781-018-0018-8.
- Bilal Alsallakh, Narine Kokhlikyan, Vivek Miglani, Shubham Mutteparwar, Edward Wang, Sara Zhang, David Adkins, and Orion Reblitz-Richardson. Debugging the internals of convolutional networks. In *Explainable AI approaches for debugging and diagnosis.*, 2021.
- G. Apollinari, I. Béjar Alonso, O. Brüning, P. Fessia, M. Lamont, L. Rossi, and L. Tavian. High-Luminosity Large Hadron Collider (HL-LHC): Technical Design Report V. 0.1. Technical report, CYRM-2017-004, 11 2017.
- Nick Cammarata, Shan Carter, Gabriel Goh, Chris Olah, Michael Petrov, Ludwig Schubert, Chelsea Voss, Ben Egan, and Swee Kiat Lim. Thread: circuits. *Distill*, 5(3):e24, 2020.
- Kipp Cannon, Sarah Caudill, Chiwai Chan, Bryce Cousins, Jolien D. E. Creighton, Becca Ewing, Heather Fong, Patrick Godwin, Chad Hanna, Shaun Hooper, Rachael Huxford, Ryan Magee, Duncan Meacher, Cody Messick, Soichiro Morisaki, Debnandini Mukherjee, Hiroaki Ohta, Alexander Pace, Stephen Privitera, Iris de Ruiter, Surabhi Sachdev, Leo Singer, Divya Singh, Ron Tapia, Leo Tsukada, Daichi Tsuna, Takuya Tsutsui, Koh Ueno, Aaron Viets, Leslie Wade, and Madeline Wade. GstLAL: A software framework for gravitational wave discovery. *SoftwareX*, 14:100680, June 2021. doi: 10.1016/j.softx.2021.100680.
- Diogo V Carvalho, Eduardo M Pereira, and Jaime S Cardoso. Machine learning interpretability: A survey on methods and metrics. *Electronics*, 8(8):832, 2019.
- Pranshu Chaturvedi, Asad Khan, Minyang Tian, E. A. Huerta, and Huihuo Zheng. Inference-optimized AI and high performance computing for gravitational wave detection at scale. *arXiv e-prints*, art. arXiv:2201.11133, January 2022.
- Yifan Chen, E. A. Huerta, Javier Duarte, Philip Harris, Daniel S. Katz, Mark S. Neubauer, Daniel Diaz, Farouk Mokhtar, Raghav Kansal, Sang Eon Park, Volodymyr V. Kindratenko, Zhizhen Zhao, and Roger Rusack. A FAIR and AI-ready Higgs Boson Decay Dataset. *arXiv e-prints*, art. arXiv:2108.02214, August 2021.
- Thomas M. Conte, Ian T. Foster, William Gropp, and Mark D. Hill. Advancing Computing’s Foundation of US Industry & Society. *arXiv e-prints*, art. arXiv:2101.01284, January 2021.
- Finale Doshi-Velez and Been Kim. Towards a rigorous science of interpretable machine learning. *arXiv preprint arXiv:1702.08608*, 2017.

- Charles A Ellis, Mohammad SE Sendi, Robyn Miller, and Vince Calhoun. A novel activation maximization-based approach for insight into electrophysiology classifiers. In *2021 IEEE International Conference on Bioinformatics and Biomedicine (BIBM)*, pages 3358–3365. IEEE, 2021.
- Dumitru Erhan, Yoshua Bengio, Aaron Courville, and Pascal Vincent. Visualizing higher-layer features of a deep network. *University of Montreal*, 1341(3):1, 2009.
- Hassan Ismail Fawaz, Germain Forestier, Jonathan Weber, Lhassane Idoumghar, and Pierre-Alain Muller. Deep learning for time series classification: a review. *Data mining and knowledge discovery*, 33(4):917–963, 2019.
- Daniel George and E. A. Huerta. Deep Learning for Real-time Gravitational Wave Detection and Parameter Estimation with LIGO Data. In *NiPS Summer School 2017*, 11 2017.
- Daniel George and E. A. Huerta. Deep neural networks to enable real-time multimessenger astrophysics. *Phys. Rev. D*, 97(4):044039, February 2018a. doi: 10.1103/PhysRevD.97.044039.
- Daniel George and E. A. Huerta. Deep Learning for real-time gravitational wave detection and parameter estimation: Results with Advanced LIGO data. *Physics Letters B*, 778:64–70, March 2018b. doi: 10.1016/j.physletb.2017.12.053.
- Daniel George and E. A. Huerta. Detecting gravitational waves in real-time with deep learning, 2018c. https://www.youtube.com/watch?v=87zE11_hkBE.
- William Gropp, Sujata Banerjee, and Ian Foster. Infrastructure for Artificial Intelligence, Quantum and High Performance Computing. *arXiv e-prints*, art. arXiv:2012.09303, December 2020.
- Dan Guest, Kyle Cranmer, and Daniel Whiteson. Deep learning and its application to lhc physics. *Annual Review of Nuclear and Particle Science*, 68(1):161–181, 2018. doi: 10.1146/annurev-nucl-101917-021019. URL <https://doi.org/10.1146/annurev-nucl-101917-021019>.
- Zhiling Guo, Sami Ullah, Antreas Afantitis, Georgia Melagraki, and Iseult Lynch. Nanotechnology and artificial intelligence to enable sustainable and precision agriculture. *Nature Plants*, 7, 06 2021. doi: 10.1038/s41477-021-00946-6.
- E. A. Huerta, Gabrielle Allen, Igor Andreoni, Javier M. Antelis, Etienne Bachelet, G. Bruce Berriman, Federica B. Bianco, Rahul Biswas, Matias Carrasco Kind, Kyle Chard, Minsik Cho, Philip S. Cowperthwaite, Zachariah B. Etienne, Maya Fishbach, Francisco Forster, Daniel George, Tom Gibbs, Matthew Graham, William Gropp, Robert Gruendl, Anushri Gupta, Roland Haas, Sarah Habib, Elise Jennings, Margaret W. G. Johnson, Erik Katsavounidis, Daniel S. Katz, Asad Khan, Volodymyr Kindratenko, William T. C. Kramer, Xin Liu, Ashish Mahabal, Zsuzsa Marka, Kenton McHenry, J. M. Miller, Claudia Moreno, M. S. Neubauer, Steve Oberlin, Alexander R. Olivas, Donald Petravick, Adam Rebei, Shawn Rosofsky, Milton Ruiz, Aaron Saxton, Bernard F. Schutz, Alex Schwing, Ed Seidel, Stuart L. Shapiro, Hongyu Shen, Yue Shen, Leo P. Singer, Brigitta M. Sipocz, Lunan Sun, John Towns, Antonios Tsokaros, Wei Wei, Jack Wells, Timothy J. Williams, Jinjun Xiong, and Zhizhen Zhao. Enabling real-time multi-messenger astrophysics discoveries with deep learning. *Nature Reviews Physics*, 1(10):600–608, October 2019. doi: 10.1038/s42254-019-0097-4.
- E. A. Huerta, Asad Khan, Edward Davis, Colleen Bushell, William D. Gropp, Daniel S. Katz, Volodymyr Kindratenko, Seid Koric, William T. C. Kramer, Brendan McGinty, Kenton McHenry, and Aaron Saxton. Convergence of Artificial Intelligence and High Performance Computing on NSF-supported Cyberinfrastructure. *Journal of Big Data*, 7(1):88, 2020. doi: 10.1186/s40537-020-00361-2.
- E. A. Huerta, Asad Khan, Xiaobo Huang, Minyang Tian, Maksim Levental, Ryan Chard, Wei Wei, Maeve Heflin, Daniel S. Katz, Volodymyr Kindratenko, Dawei Mu, Ben Blaiszik, and Ian Foster. Accelerated, scalable and reproducible AI-driven gravitational wave detection. *Nature Astronomy*, 5:1062–1068, July 2021. doi: 10.1038/s41550-021-01405-0.

- Aya Abdelsalam Ismail, Mohamed Gunady, Héctor Corrada Bravo, and Soheil Feizi. Benchmarking deep learning interpretability in time series predictions. *arXiv preprint arXiv:2010.13924*, 2020.
- Asad Khan and E. A. Huerta. Unsupervised learning and data clustering for the construction of Galaxy Catalogs in the Dark Energy Survey, 2018. <https://www.youtube.com/watch?v=n5rI573i6ws>.
- Asad Khan, E. A. Huerta, Sibor Wang, Robert Gruendl, Elise Jennings, and Huihuo Zheng. Deep transfer learning at scale for cosmology, 2018. <https://www.youtube.com/watch?v=1F3q7M8QjTQ>.
- Asad Khan, E. A. Huerta, Sibor Wang, Robert Gruendl, Elise Jennings, and Huihuo Zheng. Deep learning at scale for the construction of galaxy catalogs in the Dark Energy Survey. *Physics Letters B*, 795:248–258, August 2019. doi: 10.1016/j.physletb.2019.06.009.
- LSST Science Collaboration, P. A. Abell, J. Allison, S. F. Anderson, J. R. Andrew, J. R. P. Angel, L. Armus, D. Arnett, S. J. Asztalos, T. S. Axelrod, and et al. LSST Science Book, Version 2.0. *ArXiv e-prints*, December 2009.
- Grégoire Montavon, Alexander Binder, Sebastian Lapuschkin, Wojciech Samek, and Klaus-Robert Müller. Layer-wise relevance propagation: an overview. *Explainable AI: interpreting, explaining and visualizing deep learning*, pages 193–209, 2019.
- Akira Narita, Masao Ueki, and Gen Tamiya. Artificial intelligence powered statistical genetics in biobanks. *Journal of Human Genetics*, 66:61–65, 2020.
- Alexander H. Nitz, Tito Dal Canton, Derek Davis, and Steven Reyes. Rapid detection of gravitational waves from compact binary mergers with PyCBC Live. *Phys. Rev. D*, 98(2):024050, July 2018. doi: 10.1103/PhysRevD.98.024050.
- Michelle Ntampaka and Alexey Vikhlinin. The Importance of Being Interpretable: Toward An Understandable Machine Learning Encoder for Galaxy Cluster Cosmology. *arXiv e-prints*, art. arXiv:2112.05768, December 2021.
- Yi Pan, Alessandra Buonanno, Andrea Taracchini, Lawrence E. Kidder, Abdul H. Mroué, Harald P. Pfeiffer, Mark A. Scheel, and Béla Szilágyi. Inspiral-merger-ringdown waveforms of spinning, precessing black-hole binaries in the effective-one-body formalism. *Physical Review D*, 89(8):084006, April 2014. doi: 10.1103/PhysRevD.89.084006.
- Ramprasaath R Selvaraju, Michael Cogswell, Abhishek Das, Ramakrishna Vedantam, Devi Parikh, and Dhruv Batra. Grad-cam: Visual explanations from deep networks via gradient-based localization. In *Proceedings of the IEEE international conference on computer vision*, pages 618–626, 2017.
- Karen Simonyan, Andrea Vedaldi, and Andrew Zisserman. Deep inside convolutional networks: Visualising image classification models and saliency maps. *arXiv preprint arXiv:1312.6034*, 2013.
- Daniel Smilkov, Nikhil Thorat, Been Kim, Fernanda Viégas, and Martin Wattenberg. Smoothgrad: removing noise by adding noise. *arXiv preprint arXiv:1706.03825*, 2017.
- Mukund Sundararajan, Ankur Taly, and Qiqi Yan. Axiomatic attribution for deep networks. In *International Conference on Machine Learning*, pages 3319–3328. PMLR, 2017.
- Ian Tenney, Dipanjan Das, and Ellie Pavlick. Bert rediscovers the classical nlp pipeline. *arXiv preprint arXiv:1905.05950*, 2019.
- S. J. Tingay. An overview of the SKA project: Why take on this signal processing challenge? In *2015 IEEE International Conference on Acoustics, Speech and Signal Processing (ICASSP)*, pages 5640–5644, 2015.
- Mohammed Uddin, Yujiang Wang, and M. R. Woodbury-Smith. Artificial intelligence for precision medicine in neurodevelopmental disorders. *NPJ Digital Medicine*, 2, 2019.

- S. A. Usman et al. The PyCBC search for gravitational waves from compact binary coalescence. *Classical and Quantum Gravity*, 33(21):215004, November 2016. doi: 10.1088/0264-9381/33/21/215004.
- Michele Vallisneri, Jonah Kanner, Roy Williams, Alan Weinstein, and Branson Stephens. The LIGO Open Science Center. *J. Phys. Conf. Ser.*, 610(1):012021, 2015. doi: 10.1088/1742-6596/610/1/012021.
- Aaron van den Oord, Sander Dieleman, Heiga Zen, Karen Simonyan, Oriol Vinyals, Alex Graves, Nal Kalchbrenner, Andrew Senior, and Koray Kavukcuoglu. WaveNet: A Generative Model for Raw Audio. In *9th ISCA Speech Synthesis Workshop*, pages 125–125, 2016.
- Chelsea Voss, Gabriel Goh, Nick Cammarata, Michael Petrov, Ludwig Schubert, and Chris Olah. Branch specialization. *Distill*, 6(4):e00024–008, 2021.
- Wei Wei, E. A. Huerta, Bradley C. Whitmore, Janice C. Lee, Stephen Hannon, Rupali Chandar, Daniel A. Dale, Kirsten L. Larson, David A. Thilker, Leonardo Ubeda, Médéric Boquien, Mélanie Chevance, J. M. Diederik Kruijssen, Andreas Schrubba, Guillermo A. Blanc, and Enrico Congiu. Deep transfer learning for star cluster classification: I. application to the PHANGS-HST survey. *MNRAS*, 493(3):3178–3193, April 2020. doi: 10.1093/mnras/staa325.
- Wei Wei, Asad Khan, E. A. Huerta, Xiaobo Huang, and Minyang Tian. Deep learning ensemble for real-time gravitational wave detection of spinning binary black hole mergers. *Physics Letters B*, 812:136029, January 2021. doi: 10.1016/j.physletb.2020.136029.
- Bradley C. Whitmore, Janice C. Lee, Rupali Chandar, David A. Thilker, Stephen Hannon, Wei Wei, E. A. Huerta, Frank Bigiel, Médéric Boquien, Mélanie Chevance, Daniel A. Dale, Sinan Deger, Kathryn Grasha, Ralf S. Klessen, J. M. Diederik Kruijssen, Kirsten L. Larson, Angus Mok, Erik Rosolowsky, Eva Schinnerer, Andreas Schrubba, Leonardo Ubeda, Schuyler D. Van Dyk, Elizabeth Watkins, and Thomas Williams. Star cluster classification in the PHANGS-HST survey: Comparison between human and machine learning approaches. *MNRAS*, 506(4):5294–5317, October 2021. doi: 10.1093/mnras/stab2087.
- John R Zech, Marcus A Badgeley, Manway Liu, Anthony B Costa, Joseph J Titano, and Eric K Oermann. Confounding variables can degrade generalization performance of radiological deep learning models. *arXiv preprint arXiv:1807.00431*, 2018.